NUMERICAL MODELING OF SPACE PLASMA FLOWS// ASTRONUM-2008
Proceedings of the 2nd International Conference
ASP Conference Series, Vol. 406, 2009
Nikolai V. Pogorelov, Edouard Audit, Phillip Colella, and Gary P. Zank

Supersonically Turbulent, Shock Bound Interaction Zones

Doris Folini and Rolf Walder

École Normale Supérieure, Lyon, CRAL, UMR CNRS 5574, Université de Lyon, France

Jean M. Favre

Swiss National Supercomputing Centre (CSCS), CH-6928 Manno, Switzerland

Abstract. Shock bound interaction zones (SBIZs) are ubiquitous in astrophysics. We present numerical results for 2D and 3D, plane-parallel, infinitely extended SBIZs. Isothermal settings and parameterized cooling are considered. We highlight and compare characteristic of such zones. We emphasize the mutual coupling between the turbulence within the SBIZ and the confining shocks, point out potential differences to 3D periodic box studies of supersonic turbulence, and contemplate on possible effects on the X-ray emission of such zones.

1. Introduction

Supersonically turbulent, shock-bound interaction zones (SBIZs) are important for a variety of astrophysical objects. They contribute to structure formation in molecular clouds (Hunter *et al.* 1986; Audit and Hennebelle 2005; Vázquez-Semadeni *et al.* 2006; Hennebelle *et al.* 2008) and to galaxy formation (Anninos and Norman 1996; Kang *et al.* 2005). They affect the X-ray emission of hot-star winds (Owocki *et al.* 1988; Feldmeier *et al.* 1997) and the physics and emitted spectrum of colliding wind binaries (Stevens *et al.* 1992; Nussbaumer and Walder 1993; Myasnikov and Zhekov 1998; Folini and Walder 2000). A large number of numerical and theoretical studies have greatly improved our understanding of SBIZs under various conditions (Vishniac 1994; Blondin and Marks 1996; Walder and Folini 1998; Heitsch *et al.* 2005; Folini and Walder 2006)

In this paper, we want to highlight and compare some of the characteristics of such interaction zones under different conditions: isothermal - radiatively cooling, 2D - 3D, symmetric - asymmetric settings, early times - late times.

2. Model Problem and Numerical Method

We consider 2D and 3D, plane-parallel, infinitely extended SBIZs. Both, isothermal and radiatively cooling settings are investigated. Two high Mach-number flows, oriented parallel (left flow, subscript l) and anti-parallel (right flow, subscript r) to the x-direction, collide head on. The resulting SBIZ is oriented in the y-z-plane. It consists of a cold, dense layer (CDL) and, in the case of

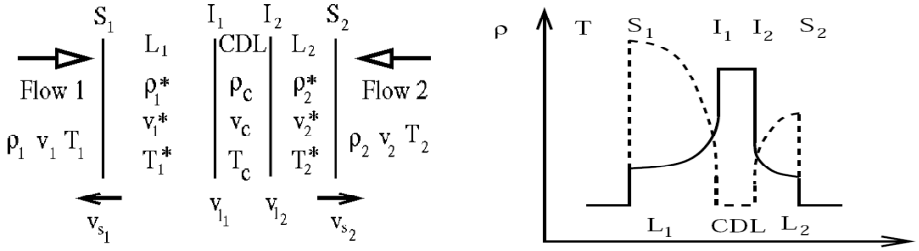

Figure 1. Sketch of the SBIZ. Radiatively cooled material piles up in the CDL. Two hot post shock layers (L1 and L2) exist in the case of parameterized cooling. Under isothermal conditions the SBIZ consists only of the CDL.

radiative cooling, two layers of hot shocked gas (Fig. 1). We investigated this system within the frame of Euler equations. In the polytropic equation of state we take $\gamma = 1.000001$ (isothermal) or $\gamma = 5/3$ (radiatively cooling). The right hand side of the energy equation we set to zero (isothermal) or to a parameterized radiative loss function (Walder and Folini 1996). Codes from the A-MAZE code package (Walder and Folini 2000a) are used. A coarse mesh is used for the upwind flows, a finer mesh for the CDL. Typical refinement factors are 2^8 in 2D and 2^4 in 3D, resulting in 1280 (2D) and 256 (3D) cells in the y-direction. The meshes adapt automatically to the spatial extension of the CDL. The solution (density) on two adjacent refinement levels is compared, cells where the difference exceeds a prescribed tolerance are flagged. Refinement is applied to rectangular blocks that contain all flagged cells and typically also some unflagged cells.

3. Characteristics of Interaction Zones

Isothermal SBIZ: Average quantities, like slab thickness, auto-correlation length of the confining shocks, or energy loss per unit volume in the CDL, evolve approximately self-similarly for symmetric flow collisions, where $\rho_\mathrm{l} = \rho_\mathrm{r} \equiv \rho_\mathrm{u}$ and $M_\mathrm{l} = M_\mathrm{r} \equiv M_\mathrm{u}$ (Folini and Walder 2006). In 2D and 3D the root mean square Mach number M_rms of the CDL scales linearly with M_u, the mean density ρ_m is independent of M_u. This contrasts with the 1D case, where $\rho_\mathrm{m} \propto M_\mathrm{u}^2$.

An intricate, 'self-regulating' interplay exists between the turbulence within the CDL and its driving: $f_\mathrm{eff} = 1 - M_\mathrm{rms}^\beta$ with $\beta \approx -0.6$ in 2D. The fraction f_eff of the upstream kinetic energy that passes the confining shocks unthermalized and M_rms affect each other. The larger M_u, the larger M_rms, and the larger the fraction of the upstream kinetic energy that is thermalized only *within* the CDL. The dependence persists for asymmetric settings, where $\rho_\mathrm{l} \neq \rho_\mathrm{r}$ and $M_\mathrm{l} \neq M_\mathrm{r}$ (Folini and Walder 2006). In 3D we find the confining shocks to be steeper than in 2D (Fig. 2, left), thus f_eff and M_rms are larger while ρ_m is smaller.

The CDL is patchy. Patch sizes increase with the x-extension of the CDL and with decreasing M_u, as does the auto-correlation length of the confining shocks. The density variance follows $\sigma^2(ln(\rho)) = ln(1 + M_\mathrm{rms}^2/4)$ (Padoan *et al.* 1997) up to $M_\mathrm{rms} \approx 5$ but then levels off (Fig. 2, right). This may be related

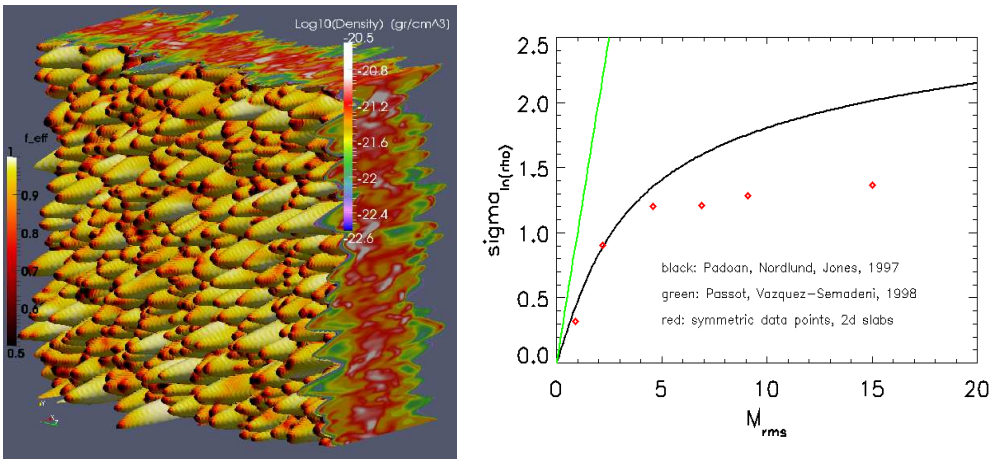

Figure 2. **Left:** Isothermal SBIZ in 3D for $M_{\rm u} = 22$. Shown is density, the confining shock is colored according to the local value of $f_{\rm eff}$. On average, the confining shocks are steeper in 3D ($f_{\rm eff} \approx 0.83$ for $M_{\rm u} = 22$) than in 2D ($f_{\rm eff} \approx 0.59$ for $M_{\rm u} = 22$). **Right:** $\sigma(ln(\rho))$ versus $M_{\rm rms}$ from 2D symmetric slab simulations (red diamonds). The 2D slab results deviate from published fitting functions by Padoan *et al.* (1997) (black) and Passot and Vázquez-Semadeni (1998) (green) for large $M_{\rm rms}$.

to the strongly anisotropic velocity field within the CDL, with larger (smaller) velocities along (perpendicular to) the upstream flow direction (Fig. 3, left).

One sided cooling SBIZ: Astrophysical examples include wind blown bubbles or planetary nebula, where a fast wind collides with a slow precursor, forming a hot ($> 10^7$ K) reverse and a cool ($< 10^6$ K) forward shock. A characteristic feature of SBIZs where one of the confining shocks cools efficiently but not the other are clumps of cold material that break off from the CDL and drift into the non-cooling, hot post-shock material (Walder and Folini 1998). Density images show a striking similarity with HST pictures of the Helix nebula. A prerequisite is that the corresponding boundary of the CDL is occasionally hit by a shock wave, which triggers a Richtmeyer-Meshkov instability. The shock wave can be generated by a thermal instability of the other hot post shock layer (Strickland and Blondin 1995; Walder and Folini 1996) or by inhomogeneities in the upstream flow. The CDL is weakly turbulent, the velocity field is isotropic.

Two sided cooling SBIZ: If both confining shocks cool efficiently with spatially resolved hot post shock layers (cooling limit = upstream temperature), the evolution of the CDL at early times can become much more violent than in the isothermal case (Fig. 4, left). At later times, the hot post shock zones rather exert a cushioning effect (Fig. 4, middle and right). The characteristics of the CDL are hardly affected. The velocity pdfs show not much change from early to late times (Fig. 3, right). Much more obvious is the difference to isothermal simulations, where the velocity field within the CDL is much more anisotropic

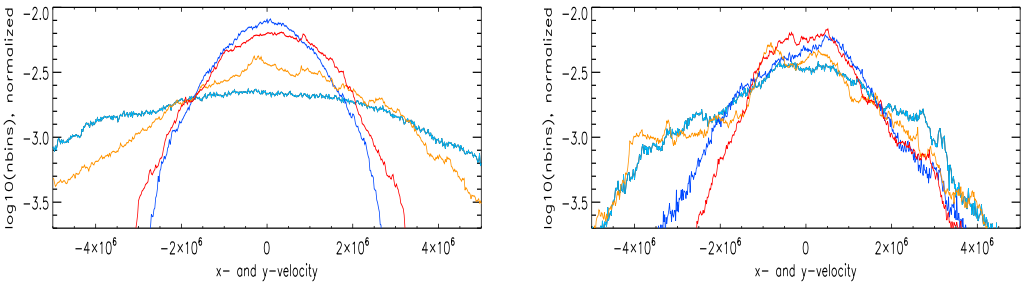

Figure 3. Velocity pdfs (x- and y-direction, two times) for an isothermal (left) and a radiatively cooling (right) 2D simulation with $M_{\rm u} = 22$ or $v_{\rm u} = 1.8 \cdot 10^7$ cm/s. An early (bluish colors) and a late time (redish colors) are shown. Wider (narrower) pdfs represent x-velocities (y-velocities). Density plots of the cooling case are shown in Fig. 4 (left and right frame).

(Fig. 3, left). Also, for the same upstream parameters, the root mean square Mach number in the CDL is much lower in the cooling case than in the isothermal case (Walder and Folini 2000b; Folini and Walder 2006). Resolved cooling layers appear to have a damping effect on the turbulence within the CDL.

4. Discussion and Conclusions

Shock bound interaction zones come in many physical varieties and an intricate interplay exists between the CDL and the confining shocks. Much work remains to be done, especially also with regard to observational and theoretical consequences. The presented results raise, in particular, the following questions.

One question concerns the wide spread assumption that the relative speed of high velocity colliding flows translates more or less directly into the hardness of the X-ray spectrum. At least under isothermal conditions the confining shocks are not perpendicular to the colliding flows but steepen with increasing $M_{\rm u}$. This should soften the spectrum and shift part of the emission from the confining shocks to internal shocks of the CDL (Smith *et al.* 2000). Whether geometrically thin, resolved cooling layers behave similarly remains to be studied.

Another topic coming to mind are the relation between SBIZs and 3D periodic box simulations. The later have enormously improved our understanding of supersonic turbulence (Mac Low 1999; Boldyrev *et al.* 2002; Padoan *et al.* 2004; Kritsuk and Norman 2004; Schmidt *et al.* 2009; Federrath *et al.* 2009). All the more one may ask to what degree these results carry over to the CDL in a SBIZ, where surface effects play a role. Three points may be raised.

In an isothermal SBIZ, $M_{\rm rms}$, the energy input into the CDL, and the spatial scale on which this energy input is modulated all depend on each other. In 3D box simulations, the energy input and its spatial modulation - the driving wave length - are usually chosen independently. The effect of this difference on the turbulence characteristics remains to be clarified. A second point is the velocity field, which is clearly anisotropic in the CDL but usually isotropic by design in 3D box simulations. Finally, when computing a CDL-averaged structure function (SF) for our 3D CDL (compute SFs for each point in the CDL, using only points

in the CDL, then taking the average over all SFs) it resembles more closely the observation based SFs by Gustafsson *et al.* (2006) than those typically found for 3D boxes (Boldyrev *et al.* 2002; Padoan *et al.* 2004; Kritsuk and Norman 2004). The reason is not yet clear. It could be the finite spatial extension of the CDL, its inhomogeneous, anisotropic interior, or simply a too coarse resolution.

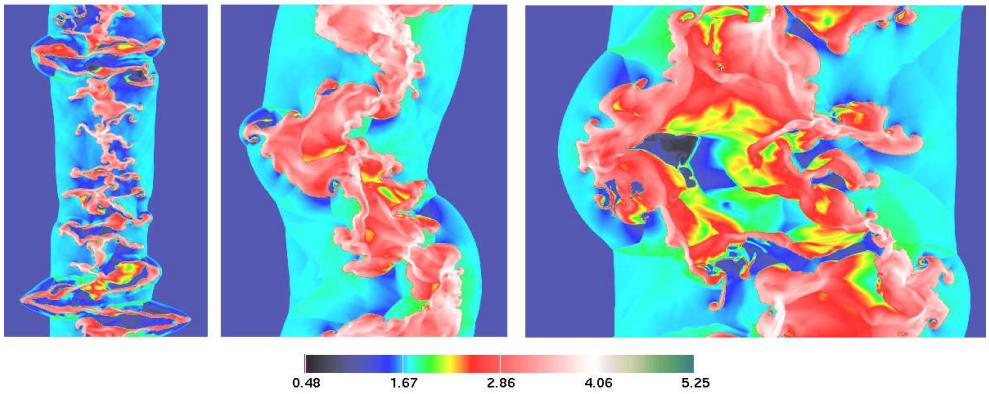

Figure 4. Two sided cooling SBIZ, time evolution, logarithm of density. CDL in red and white, hot post shock layers in light blue. Filamentary and dynamic at early times, the CDL becomes more 'bulky' later on. Nevertheless, small scale features at the surface of the CDL continue to form and vanish. No CDL was present at time 0.

Further studies of SBIZs are needed, both with basic physics and with more elaborate models, and with particular attention to the interplay between the confining shocks and the turbulent CDL.

Acknowledgments. The authors wish to thank the crew running the HP Superdome at ETH Zurich and the people of the Swiss Center for Scientific Computing, CSCS Manno, where the simulations were performed. The authors much appreciated the stimulating discussions during ASTRONUM, in particular with E. Audit, P. Hennebelle, A. Kritsuk, and W. Schmidt.

References

Anninos, P. and Norman, M. L. (1996). The role of hydrogen molecules in the radiative cooling and fragmentation of cosmological sheets. *ApJ*, **460**, 556–568.

Audit, E. and Hennebelle, P. (2005). Thermal condensation in a turbulent atomic hydrogen flow. *A&A*, **433**, 1–13.

Blondin, J. M. and Marks, B. S. (1996). Evolution of cold shock-bounded slabs. *New Astronomy*, **1**, 235–244.

Boldyrev, S., Nordlund, Å., and Padoan, P. (2002). Scaling Relations of Supersonic Turbulence in Star-forming Molecular Clouds. *ApJ*, **573**, 678–684.

Federrath, C., Klessen, R. S., and Schmidt, W. (2009). The Fractal Density Structure in Supersonic Isothermal Turbulence: Solenoidal Versus Compressive Energy Injection. *ApJ*, **692**, 364–374.

Feldmeier, A., Puls, J., and Pauldrach, A. W. A. (1997). A possible origin for X-rays from O stars. *A&A*, **322**, 878–895.

Folini, D. and Walder, R. (2000). Theory of Thermal and Ionization Effects in Colliding Winds of WR+O Binaries. In *ASP Conf. Ser. 204: Thermal and Ionization Aspects of Flows from Hot Stars*, pages 267–280.

Folini, D. and Walder, R. (2006). Supersonic turbulence in shock-bound interaction zones. I. Symmetric settings. *A&A*, **459**, 1–19.

Gustafsson, M., Brandenburg, A., Lemaire, J. L., and Field, D. (2006). The nature of turbulence in OMC1 at the scale of star formation: observations and simulations. *A&A*, **454**, 815–825.

Heitsch, F., Burkert, A., Hartmann, L. W., Slyz, A. D., and Devriendt, J. E. G. (2005). Formation of Structure in Molecular Clouds: A Case Study. *ApJ*, **633**, L113–L116.

Hennebelle, P., Banerjee, R., Vázquez-Semadeni, E., Klessen, R. S., and Audit, E. (2008). From the warm magnetized atomic medium to molecular clouds. *A&A*, **486**, L43–L46.

Hunter, J. H., Sandford, M. T., Whitaker, R. W., and Klein, R. I. (1986). Star formation in colliding gas flows. *ApJ*, **305**, 309–332.

Kang, H., Ryu, D., Cen, R., and Song, D. (2005). Shock-heated Gas in the Large-Scale Structure of the Universe. ApJ, **620**, 21–30.

Kritsuk, A. G. and Norman, M. L. (2004). Scaling Relations for Turbulence in the Multiphase Interstellar Medium. *ApJ*, **601**, L55–L58.

Mac Low, M.-M. (1999). The Energy Dissipation Rate of Supersonic, Magnetohydrodynamic Turbulence in Molecular Clouds. *ApJ*, **524**, 169–178.

Myasnikov, A. V. and Zhekov, S. A. (1998). Dissipative models of colliding stellar winds - I. Effects of thermal conduction in wide binary systems. *MNRAS*, **300**, 686–694.

Nussbaumer, H. and Walder, R. (1993). Modification of the nebular environment in symbiotic systems due to colliding winds. *A&A*, **278**, 209–225.

Owocki, S. P., Castor, J. I., and Rybicki, G. B. (1988). Time-dependent models of radiatively driven stellar winds. I - Nonlinear evolution of instabilities for a pure absorption model. *ApJ*, **335**, 914–930.

Padoan, P., Nordlund, A., and Jones, B. J. T. (1997). The universality of the stellar initial mass function. *MNRAS*, **288**, 145–152.

Padoan, P., Jimenez, R., Nordlund, Å., and Boldyrev, S. (2004). Structure Function Scaling in Compressible Super-Alfvénic MHD Turbulence. *Physical Review Letters*, **92**(19), 191102–+.

Passot, T. and Vázquez-Semadeni, E. (1998). Density probability distribution in one-dimensional polytropic gas dynamics. *Physical Review Letters*, **58**, 4501–4510.

Schmidt, W., Federrath, C., Hupp, M., Kern, S., and Niemeyer, J. C. (2009). Numerical simulations of compressively driven interstellar turbulence. I. Isothermal gas. *A&A*, **494**, 127–145.

Smith, M. D., Mac Low, M.-M., and Heitsch, F. (2000). The distribution of shock waves in driven supersonic turbulence. *A&A*, **362**, 333–341.

Stevens, I. R., Blondin, J. M., and Pollock, A. M. T. (1992). Colliding winds from early-type stars in binary systems. *ApJ*, **386**, 265–287.

Strickland, D. and Blondin, J. M. (1995). Numerical analysis of the dynamic stability of radiative shocks. *ApJ*, **449**, 727–738.

Vázquez-Semadeni, E., Ryu, D., Passot, T., González, R. F., and Gazol, A. (2006). Molecular Cloud Evolution. I. Molecular Cloud and Thin Cold Neutral Medium Sheet Formation. *ApJ*, **643**, 245–259.

Vishniac, E. T. (1994). Nonlinear instabilities in shock-bounded slabs. *ApJ*, **428**, 186–208.

Walder, R. and Folini, D. (1996). Radiative cooling instability in 1D colliding flows. *A&A*, **315**, 265–283.

Walder, R. and Folini, D. (1998). Knots, filaments, and turbulence in radiative shocks. *A&A*, **330**, L21–L24.

Walder, R. and Folini, D. (2000a). A-MAZE: A code package to compute 3D magnetic flows, 3D NLTE radiative transfer, and synthetic spectra. In H. J. G. L. M. Lamers and A. Sapar, editors, *Thermal and Ionization Aspects of Flows from Hot Stars: Observations and Theory*, ASP Conference Series, pages 281–285.

Walder, R. and Folini, D. (2000b). On the Stability of Colliding Flows: Radiative Shocks, Thin Shells, and Supersonic Turbulence. *Ap&SS*, **274**, 343–352.